This is an author's version published in: http://oatao.univ-toulouse.fr/21841

Carbon dioxide gas hydrate crystallization in porous silica gel particles partially saturated with a surfactant solution

Christophe Dicharry [a,*], Christophe Duchateau [b], Halim Asbaï [a],
Daniel Broseta [a], Jean-Philippe Torré [a]

[a] Univ. Pau & Pays Adour, CNRS, TOTAL–UMR 5150–LFC-R–Laboratoire des Fluides Complexes et leurs Réservoirs,
Avenue de l'Université, BP 1155–PAU, F-64013, France
[b] Stanford University, Energy Resources Engineering, 367 Panama St., Stanford, CA 94305, USA

- High water to hydrate conversion can be achieved in silica gel particles.
- Sodium dodecyl sulfate (SDS) enhances CO_2 hydrate formation in silica gel particles.
- In the presence of SDS, CO_2 hydrate first forms in the bulk water phase.

This paper reports on investigations into the way carbon dioxide (CO_2) hydrate forms in porous silica gel partially saturated with pure water or with a surfactant solution. The experiments, conducted at two different temperatures (278.2 and 279.2 K) and under a loading pressure of 3.8 MPa, used silica particles of different nominal pore diameters (30 and 100 nm), saturated at 80% pore volume with pure water or with a 100 ppm solution of either sodium dodecyl sulfate (SDS) or polyoxyethylenesorbitan monoleate (Tween 80). They were run following the "hydrate precursor method" developed in previous works (Duchateau et al., 2009, 2010) to form *bulk* hydrate under controlled subcooling conditions, and adapted for studying hydrate formation behavior in porous media.

The work demonstrated that the successive hydrate formation and decomposition cycles involved in this method do not alter the pore size distribution in the porous media. At the two temperatures investigated, silica gel particles with a nominal pore diameter of 100 nm proved better suited to comparing the CO_2 hydrate formation behaviors: higher water to hydrate conversions (> 90 mol%) were effectively obtained for all the conditions tested making comparison of the results much easier. Of the two surfactants used, only SDS was found to produce a positive effect on both the hydrate formation kinetics and the amount of hydrate formed. Our visual observations of quiescent bulk systems (without porous silica gel) suggest that when SDS is present, CO_2 hydrate forms not only at the w/g interface (where it occurs without SDS too), but also in the bulk water phase. This may explain the beneficial effect observed on the porous medium.

1. Introduction

Gas hydrates are clathrate solids composed of cavities formed of hydrogen bonded water molecules, which can accommodate differ ent sized gas molecules (Sloan and Koh, 2008). They may form when water and gas molecules are present under thermodynamically suitable conditions, i.e. at low enough temperatures and high enough pressures. Several gas hydrate properties have attracted the attention of the scientific and industrial communities for their potential in such practical applications as refrigeration and air conditioning (Delahaye et al., 2011; Darbouret et al., 2005), energy storage or transportation (Gudmundsson et al., 1999; Belosludov et al., 2007), or capture of greenhouse gases (Adeyemo et al., 2010; Seo et al., 2005; Ricaurte et al., 2011). Those properties include a high latent heat of melting, and the capacity not only to encapsulate large amounts of gas (if all the cavities are filled, each volume of CO_2 hydrate may contain 175 volumes of CO_2 at standard temperature and pressure (Sloan and Koh, 2008)) but also to selectively capture certain components in gas mixtures.

Depending on the target application of gas hydrates, different key issues, such as the selectivity of the enclathration process, the amount of gas hydrate formed and the transportability of gas

hydrates, need to be addressed. One of the technological bottlenecks (to make any hydrate based process economically viable) centers on the kinetics of hydrate formation: the formation rate of gas hydrates is generally slow as the reaction usually takes place, or at least starts, at the water/gas (w/g) interfaces (Englezos et al., 1987; Ohmura et al., 2000). The barrier formed as the hydrate crystals grow and agglomerate at these interfaces impedes transfer from the gas phase to the hydrate forming phase. Crystallization is drastically decreased (and sometimes completely halted) once the w/g interface becomes totally crusted in hydrate, preventing any substantial level of water to hydrate conversion from being reached.

One strategy for improving the kinetics of hydrate formation is therefore to increase the area of the w/g interface available for the hydrate reaction. This can be done in different ways, such as vigorously mixing the water and gas phases, spraying water in the gas phase, bubbling the gas phase in water, or using a porous medium saturated with water. Another strategy is to use chemical additives, such as thermodynamic hydrate promoters (e.g. tetra hydrofuran (THF), or alkyl ammonium salts) (Kang et al., 2001; Torré et al., 2011; Mohammadi et al., 2012; Sun et al., 2011), or kinetic hydrate promoters, generally surfactants (e.g. sodium dodecyl sulfate, SDS) (Zhong and Rogers, 2000; Gayet et al., 2005), or a mixture of the two (Zhu et al., 2011; Torré et al., 2012).

The use of a porous medium, such as silica gel particles fully or partially saturated with water, may be an interesting approach. The gas phase can circulate through the interparticular porosity (macroporosity), making for a large available exchange surface between pore water and gas that enhances the hydrate formation kinetics and the water to hydrate conversion rate (Kang and Lee, 2010; Kumar et al., 2013). Further benefits of using a porous medium include: no hydrate slurry to handle (and therefore no risk of hydrate particles agglomerating and plugging the flow lines), no additional power consumption required to generate the w/g interface, and improved process safety conditions (gas leakage problems are reduced by the absence of the agitator gland packing needed to seal the shaft of mechanical agitation systems).

Recent research works on hydrate crystallization in porous media address the effect of water confinement on hydrate phase equilibrium, on the kinetics of hydrate formation and on the water to hydrate conversion ratio under different experimental conditions (pore and particle size, pressure, temperature, etc). However, few studies have been published on the effect on the above parameters of adding hydrate promoters — and more specifically kinetic hydrate promoters — to the pore water. To the best of our knowledge, only Kang and Lee (2010), and very recently Kumar et al. (2013), have studied the effect of kinetic promoters (surfactants) on the kinetics of CO_2 hydrate formation in porous media. On the one hand, Kang and Lee (2010) evaluated the promotional effect of SDS on the formation behavior of this hydrate in spherical silica gel with a nominal pore diameter of 100 nm for different pressure and temperature conditions and different concentrations of SDS. They found that in the presence of SDS, both the initial formation rate and the final gas consumption parameters generally increase with the driving force imposed to form the hydrate, and that the time lapse (i.e. the induction time) usually observed for hydrate formation is considerably reduced. They also observed that an SDS concentration of 100 ppm produces the highest values for the above two parameters whereas the beneficial effect decreases at higher concentration. On the other hand, Kumar et al. (2013) used three different kinds of surfactants — SDS for the anionic surfactant, DATCl for the cationic surfactant and Tween 80 for the nonionic surfactant — and porous media of very similar pore diameter (~60 Å) but different surface area. They found SDS to be the most effective in enhancing the rate of hydrate formation and reducing the induction time, and DATCl to exhibit a certain inhibition effect on hydrate formation. The

optimum concentration for SDS and Tween 80 was estimated to be 4000 and 2000 ppm, respectively. Interestingly, SDS and Tween 80 appeared to have little effect on the total amount of hydrate formed, as compared to the same system with no surfactant.

Owing to the widely dispersed experimental results typical of crystallization phenomena, additional experimental data are needed to determine whether there is a synergetic effect between the presence of a kinetic promoter and the high exchange surface available between pore water and gas in the porous medium. As a contribution to meeting that need, we studied the formation kinetics and the amount of CO_2 hydrate formed in porous media of nominal pore diameter 30 nm and 100 nm, with and without SDS and Tween 80. The experiments presented here were conducted under isochoric conditions, at the two different temperatures imposed for hydrate formation. The Experimental section (Section 2) of this article, below, presents a specific protocol developed to control the temperature at which hydrate formation starts. Based on the "water memory" effect, the protocol takes advantage of the residual structures remaining in solution after a prior hydrate formation/decomposition cycle to reduce the stochastic character of hydrate crystallization in subsequent formations (Duchateau et al., 2010; Adeyemo et al., 2010). It also ensures that hydrate formation begins within a reasonable time after the target temperature is reached. Each experiment reported in this study has generally been triplicated in order to assess the reproducibility of the results obtained.

2. Experimental section

2.1. Materials

CO_2 gas (purity of 99.995 mol%) was supplied by Linde gas. The chemicals used as kinetic hydrate promoters were: sodium dodecyl sulfate (SDS) from Chem Lab (purity > 98%) and polyoxyethylenesorbitan monoleate (Tween 80) from Sigma Aldrich (purity > 99.9%). The aqueous solutions were prepared using ultra pure water (resistivity of 18.2 MΩ cm). Both surfactants were used at a concentration of 100 ppm (by weight).

The porous media were spherical silica gel particles purchased from Silicycle (Canada). Table 1 summarizes their main properties.

2.2. Apparatus

A schematic illustration of the experimental setup used in this study is shown in Fig. 1. It consists of three 316 stainless steel high pressure cells with an internal volume of 128.0 ± 0.5 cm^3 immersed in a fully insulated temperature controlled bath agitated with two impellers to provide homogeneous temperature control during the experiments. Bath temperature is regulated by an electric heater (from MGW Lauda) driven by a Shimaden SR53 programmable temperature controller and a cryostat (F32 HE model from Julabo). Each cell is connected to a CO_2 supply vessel that loads the gas into the cell at the required pressure.

The temperature in the cells and bath is measured using PT100 probes with an accuracy of ± 0.2 K, while pressure in the cells is measured with 10 MPa full scale transducers with a precision of

Table 1
Physical properties of the silica gels used in this study.

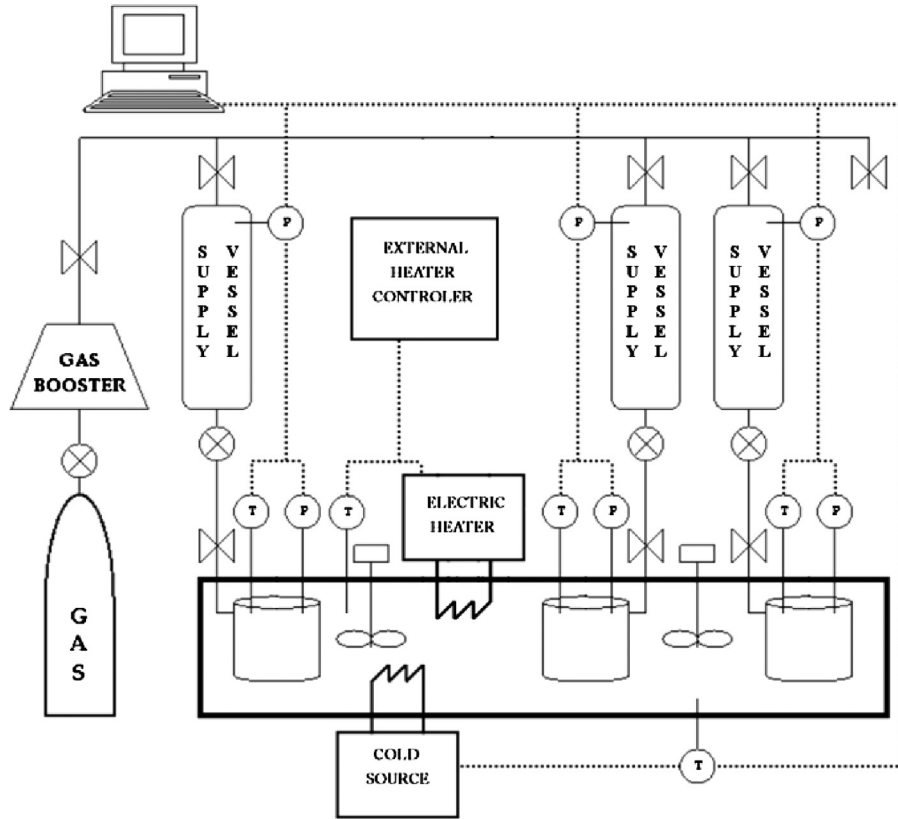| Sample name	SG30	SG100
Mean particle diameter (μm)	20–45	20–45
Mean pore diameter (nm)	30	100
Pore volume (mL/g)	0.80	0.76
Surface area (m^2/g)	109	30

Fig. 1. Schematic representation of the apparatus.

0.3% FS. Pressure and temperature are recorded every minute by a computer running a specific SpecView© application.

2.3. Procedure for hydrate formation experiments

For each experiment, the cells were loaded with a given mass of silica gel particles (dried at 393 K for 24 h beforehand), after which a quantity of aqueous solution (with or without SDS or Tween 80 present) calculated to saturate 80% of the available pore volume was poured onto the powder. The cells were then closed, immersed into the temperature controlled bath and connected to the CO_2 supply vessels. They were purged twice with CO_2 to remove the remaining air in the system and pressurized with about 3.8 MPa of CO_2 at 283.2 K (these pressure and temperature conditions are outside the CO_2 hydrate stability zone). The systems were then left overnight at this temperature to let the CO_2 solubilize in the pore water.

All experiments were conducted under isochoric conditions; the total quantity of matter present in the cell was therefore constant throughout the experiment.

The procedure we used here to form hydrates in porous media at a target temperature T_{targ} is schematically depicted in Fig. 2. It is very similar to the so called "hydrate precursor method" developed previously in our laboratory for testing kinetic hydrate inhibitors in the absence of a porous medium (in the *bulk* as this situation is referred to below) (Duchateau et al., 2009, 2010). It consists in forming hydrate with a water phase that has previously experienced hydrate formation and decomposition. As demonstrated in our previous works, the melted hydrates leave a number of residual structures in the water that not only promote subsequent hydrate formation i.e. the hydrate re formation temperature $T_{re-form}$ is higher and the hold time t_{hold} is shorter but also drastically increase the repeatability of these two parameters. The hold time is defined as the difference between the onset of hydrate (re)formation and the time at which the system enters the hydrate stability zone.

In the present study, the first hydrate crystallization (first stage in Fig. 2) was achieved by rapidly cooling the equilibrated system from $T_{init}=283.2$ K to $T_1=269.2$ K. The temperature was then raised to $T_2=275.2$ K (still inside the CO_2 hydrate stability zone but above the ice melting temperature) and maintained at this value for at least 4 h in order to melt and convert to hydrate any ice that might have crystallized at T_1. On completion of this stage, we expected to find almost the same amount of CO_2 hydrate formed in each cell. After the pressure stabilized, the system was heated at a rate of 0.9 K/h to a temperature T_d just above $T_{eq}=281.9$ K (the CO_2 hydrate equilibrium temperature at 3.8 MPa) where it was left for $t_d=4$ h to melt the CO_2 hydrate (second stage in Fig. 2). It was then cooled to 274.2 K at a rate of 4 K/h (left side of the third stage in Fig. 2). Hydrate re formation usually occurred during the cooling ramp, at $T_{re-form}$ indicated by a sudden increase in the temperature profile due to the exothermic character of hydrate crystallization.

By varying T_d (from 282.3 to 284.1 K) in the second stage of the procedure and determining the corresponding $T_{re-form}$ for a set of experiments, we were able to plot a $T_{re-form}$ vs. T_d chart. Fig. 3 (a) shows the chart obtained for the SG30 porous medium partially (80%) saturated with a 100 ppm Tween 80 solution. Fig. 3(b) shows, for the same system, the variation of $T_{re-form}$ as a function of t_d, at $T_d=283.2$ K. Each point in Fig. 3(a) and (b) averages at least three experimental values, and the error bars represent the difference between the extreme and mean values.

The $T_{re-form}$ vs. T_d curve (Fig. 3(a)) follows the trend already observed for bulk systems in our previous work (Duchateau et al., 2010), i.e. as T_d increases, both the average value and the reproducibility of $T_{re-form}$ decrease. $T_{re-form}$ shows the same ten dency when t_d is varied (Fig. 3(b)) at a constant temperature for hydrate melting (here 283.2 K). Therefore, like the observations in *bulk* systems, history effects are also found when hydrate is decomposed in porous media in the immediate vicinity of the phase boundary.
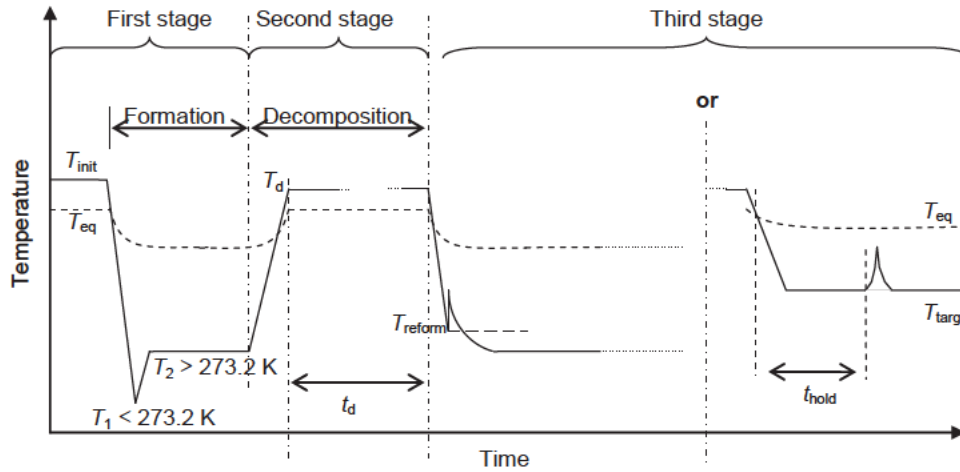
Fig. 2. Experimental procedure.
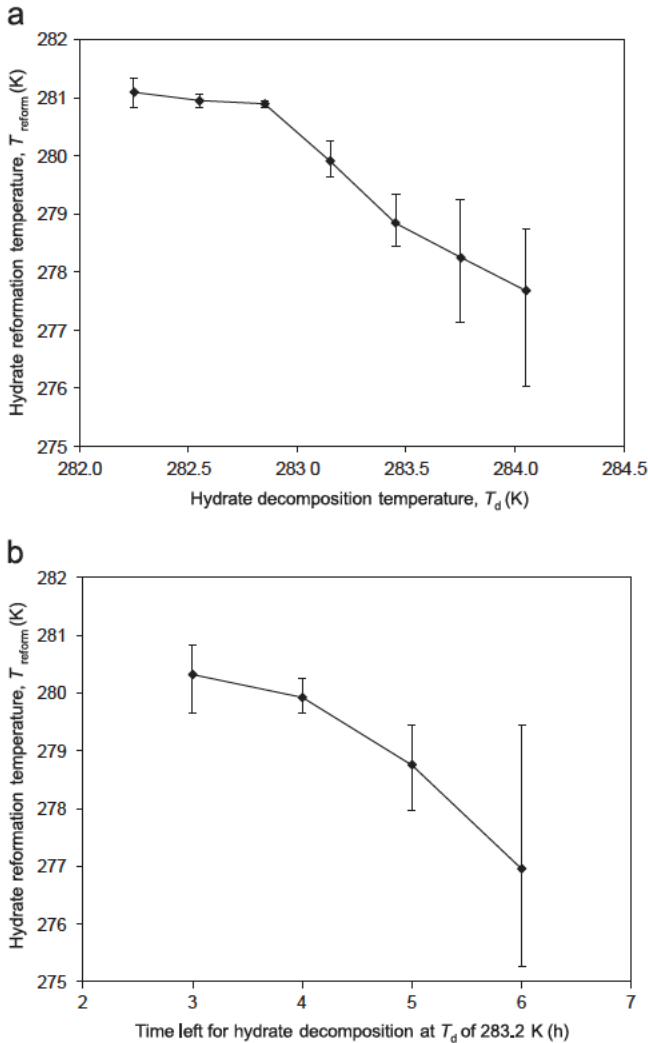

a

b

Fig. 3. (a) Hydrate re-formation temperature as a function of the temperature set to melt hydrate (the time left for hydrate decomposition is 4 h), and (b) hydrate re-formation temperature as a function of the time left for hydrate decomposition at T_d 283 K for the SG30 porous medium partially (80%) saturated with a 100 ppm Tween-80 aqueous solution.

The $T_{re-form}$ vs. T_d chart (Fig. 3(a)) can be used as a guideline to find the decomposition temperature to impose on the system in order to obtain hydrate re crystallization once the desired tem perature has been reached (right side of the third stage in Fig. 2).

For example, for the SG30 porous medium with Tween 80, hydrate re crystallization is expected to occur at a temperature of about 279 K if the hydrate formed in the first stage of the procedure is melted for $t_d = 4$ h at 283.5 K.

To summarize, the three stages of the "hydrate precursor method" applied to form CO_2 hydrate in the porous medium at a desired temperature are: (i) an initial hydrate crystallization is imposed on the system, (ii) hydrate is melted for 4 h at a temperature T_d chosen from the $T_{re-form}/T_d$ chart, and then, (iii) the system is cooled to a temperature (T_{targ}) a little higher (~ 0.2 K) than the $T_{re-form}$ corre sponding to T_d on the $T_{re-form}/T_d$ chart.

By applying this procedure, hydrate generally re formed within a few hours after the temperature stabilized at T_{targ}.

3. Results and discussion

3.1. Integrity of the porous medium subjected to consecutive hydrate formation/decomposition cycles

Because the "hydrate precursor method" implies an initial hydrate formation and decomposition, we first investigated the effect of successive formation/decomposition cycles on the integrity of the porous media used. Fig. 4(a) shows in a P T diagram the hysteresis curves obtained for three cycles in the SG30 porous medium with pure water. From point A (initial P T conditions), the system is quickly cooled until hydrate is formed (point B, B' or B"). Note that to force the initial hydrate formation (point B) to occur, we had to impose a temperature lower than ice equilibrium temperature. The tempera ture of the system was then set at 274.2 K (or 275.2 K, in order to gain time in the third experiment) (point C) where it was maintained for several hours until the pressure stabilized. From points C to F, the system was heated at a constant rate of 0.1 K/h. Because the phase equilibrium of hydrates confined in pores of small diameter shifts to lower temperatures and higher pressures compared to bulk hydrates (Handa and Stupin, 1992), CO_2 hydrate decomposes first in the pores of smallest diameter and then progressively through the bigger sized pores as the temperature of the system increases. Hydrate decom position is completed at point D, which corresponds to the hydrate dissociation in the largest pores filled with CO_2 hydrate. By then, further heating to point F results in a small linear pressure rise caused by gas expansion with temperature.

The elongated S shape of the heating curve between points C and D essentially reflects the cumulative pore volume distribution of the porous medium used (Dicharry et al., 2005). It is clear in Fig. 4(a) that the three heating curves between C and F super impose perfectly, suggesting that the volume expansion that occurs when porous water is converted to hydrate does not alter
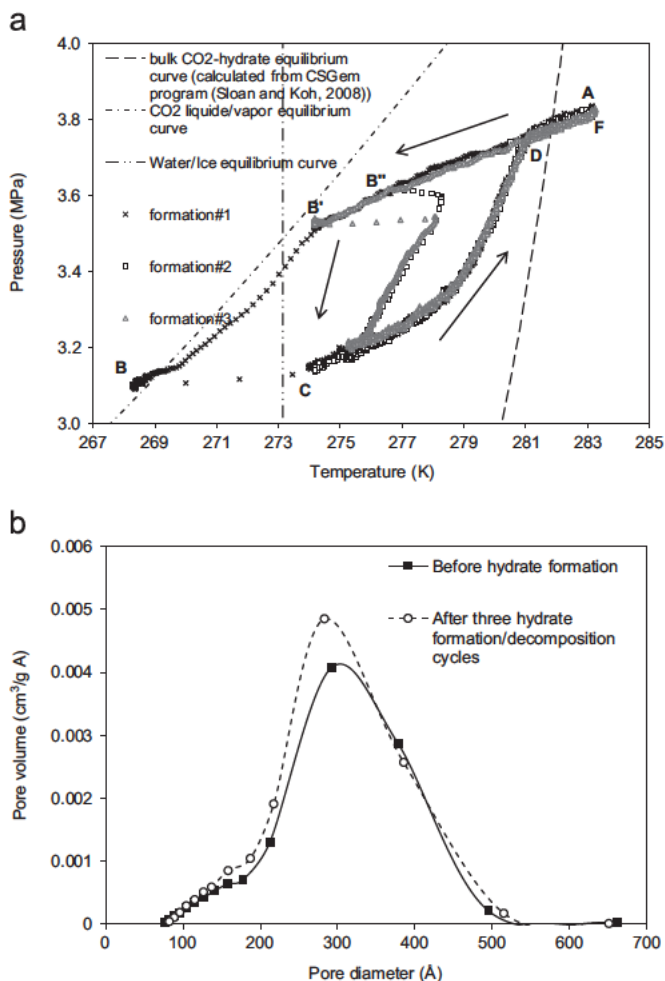
Fig. 4. (a) Hysteresis curves obtained for three hydrate formation/decomposition cycles with the SG30 porous medium partially (80%) saturated with pure water, and (b) pore size distribution of the SG30 porous medium before and after the three hydrate formation/decomposition cycles.

the pore size distribution (PSD) in the medium used. This point was confirmed by measuring (by nitrogen adsorption/desorption experiments with an ASAP 2020 gas sorption analyzer from Micromeritics) and comparing the PSD of SG30 samples before and after three hydrate formation/decomposition cycles (Fig. 4(b)).

3.2. Hydrate formation in the porous media partially (80%) saturated with pure water: effect of pore size distribution

In this part of the work, the CO_2 hydrate is formed in the SG30 and SG100 porous media at two different temperatures (278.2 and 279.2 K), using the experimental procedure described in Section 2. In each case, hydrate crystallization occurred after the temperature of the system reached the target value. Fig. 5(a) and (b) shows the pressure decrease measured in the cell as a function of time for the SG30 and SG100 porous media, respectively. Each experiment was duplicated.

The reproducibility of the experiments performed at a given temperature is very good. When the temperature imposed for hydrate formation varies, drastic differences are observed between the two systems.

For the SG30 porous medium, the total pressure decrease strongly depends on the temperature at which the hydrate is formed: the pressure decreases are approx. 0.05 MPa at 279.2 K and 0.3 MPa at 278.2 K. The difference reflects the different amounts of water converted to hydrate. It results from both the hydrate equilibrium

pressure, which varies with the temperature imposed to form the hydrate, and the distribution of the hydrate equilibrium conditions due to the PSD of the porous medium. When the temperature applied to form hydrate changes, the minimum pore diameter below which hydrate cannot form also changes. Fig. 6 depicts schematically the effects observed. The full lines plotted in Fig. 6(a) correspond to the hydrate equilibrium curves for bulk hydrate and for the hydrate confined in pores of diameters d_{min} and d_{max} (the extreme diameters of the PSD for the considered porous medium). Note that if d_{max} is large enough (typically larger than 500 nm), the hydrate equilibrium conditions in pores of this diameter should coincide with those of bulk hydrate (Turner et al., 2005). When the temperature of the system is set at T_1, the pressure at equilibrium will take a value P_1, which corresponds to the hydrate equilibrium pressure for the pores of diameter d_1. Under these conditions, the hydrate is present and stable only in the pores with diameters between d_1 and d'_{max} (shaded area in Fig. 6(b)), d'_{max} being the diameter of the largest pores initially filled with water (in our case, d'_{max} is smaller than d_{max} since only 80% of the available pore volume is saturated with water). Starting from the same initial conditions, if the temperature is set at T_2 ($>T_1$), the pressure at equilibrium will then take a value P_2 ($>P_1$) corresponding to the hydrate equilibrium pressure for pores of diameter d_2 ($>d_1$). In this case, the hydrate is present and stable in the pores with diameters between d_2 and d'_{max} (shaded area in Fig. 6 (c)), and the total amount of hydrate formed will therefore be smaller than in the former case.
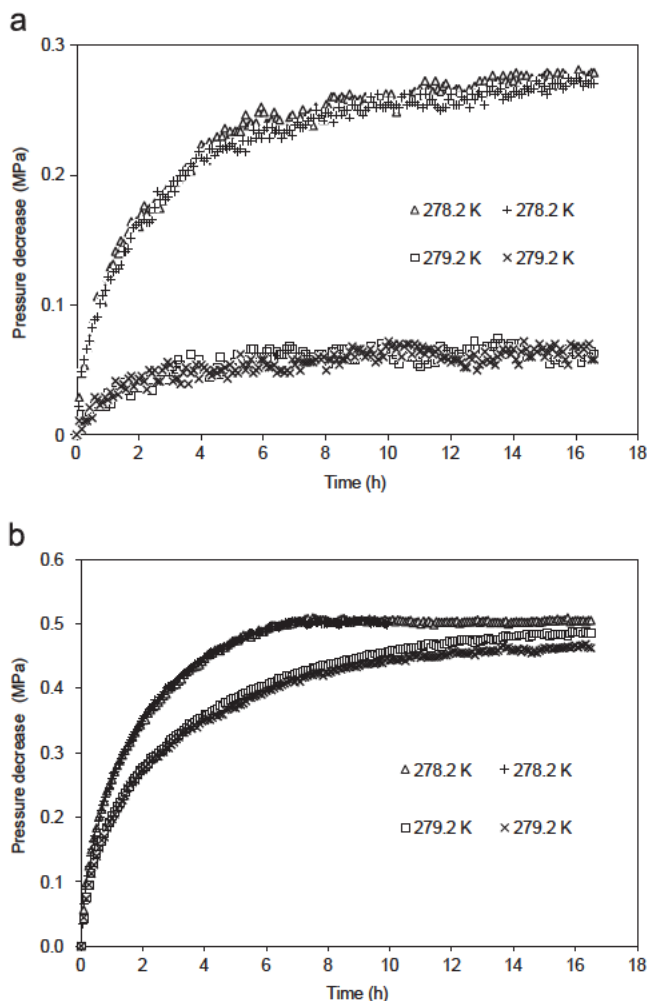

Fig. 5. Pressure decrease as a function of time: (a) for the SG30, and (b) the SG100 porous media partially (80%) saturated with pure water, at two different temperatures imposed for hydrate formation.
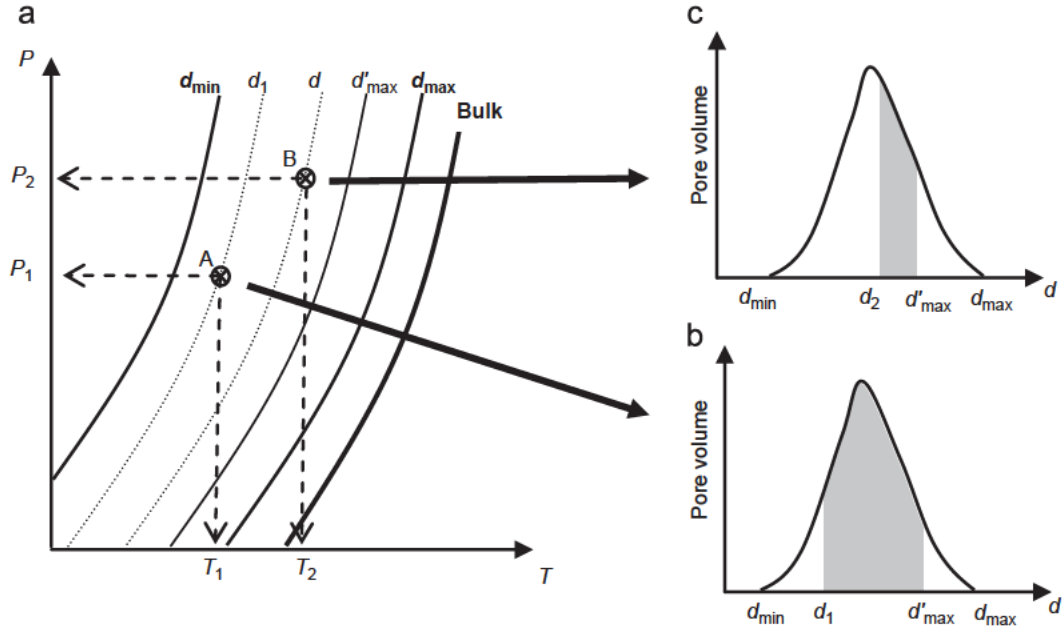
Fig. 6. Schematic description of the effect of pressure and temperature conditions on the amounts of hydrate formed in the porous medium: (a) representation of the hydrate equilibrium phase boundary for different pore diameters and for bulk in a P–T diagram, (b) and (c) show the fraction of the pore size distribution occupied by hydrate (shaded area), at (P_1,T_1) and (P_2,T_2), respectively.

The large diameters of the pores present in the SG100 porous medium imply that the equilibrium conditions for hydrates formed there are closer to bulk hydrate conditions than those for hydrates formed in the SG30 porous medium. As a consequence, at both temperatures investigated in this study, CO_2 hydrate formed in most of the pores in the SG100 porous medium containing water. However, the temperature of 278.2 K allows the hydrate to form in pores of smaller diameters than at 279.2 K, as reflected by the slightly higher pressure decrease observed.

The amount of hydrates formed varies considerably with the temperature applied in the SG30 porous medium, making it difficult to compare the kinetics of hydrate formation easily. So, in the rest of this paper, we will describe and discuss only the results obtained with the SG100 porous medium.

3.3. Hydrate formation in the SG100 porous medium partially (80%) saturated with a surfactant solution

In these experiments, 80% of the available pore volume in the SG100 porous medium was saturated with a solution of Tween 80 or SDS at a concentration of 100 ppm. As in the previous paragraph, the "hydrate precursor method" was used to form CO_2 hydrate in the porous medium at two different temperatures (278.2 and 279.2 K). Fig. 7(a) and (b) shows the pressure decrease measured in the cell as a function of time. Each experiment was duplicated. The insets in Fig. 7(a) and (b) give a detailed view of the pressure decrease that occurs in the first 3 h of hydrate formation. For clarity, the experimental results with pure water (shown in Fig. 5(b)) are not superimposed over the data but their envelope is displayed in the insets of Fig. 7.

Table 2 shows the formation behaviors and equilibrium data of CO_2 hydrate in the SG100 porous medium with the surfactant solutions and pure water. The data presented are: (i) the total pressure decrease, ΔP_f obtained at the end of the experiment, (ii) $t_{50\%}$ and $t_{90\%}$, the time necessary for the pressure decrease to reach 50% and 90% of ΔP_f respectively the time $t=0$ was taken at the onset of hydrate growth and (iii) R_f, the initial hydrate formation rate, calculated as the initial slope of the 6° polynomial fit of the first 3 h pressure decrease vs. time curve, and (iv) τ_w, the molar ratio of water to hydrate at final conversion.

τ_w was calculated using the following equation:

$$\tau_w = \frac{\Delta n_{CO_2}^h \times N_h}{n_w} \tag{1}$$

where $\Delta n_{CO_2}^h$ is the total number of moles of gas consumed for hydrate formation, N_h the hydration number and n_w the total number of moles of water.

Here, $\Delta n_{CO_2}^h$ was calculated as the variation of the number of moles of CO_2 in the gas phase, $\Delta n_{CO_2}^g$ (deduced from the pressure drop at the temperature T_{targ} imposed for hydrate formation (278.2 or 279.2 K)) plus the number of moles of CO_2 solubilized in the aqueous phase, $n_{CO_2}^w(T_{targ},P)$ at the gas pressure P measured before hydrate formation at T_{targ}. Of course, the assumption that all the moles of CO_2 present in the water phase have been consumed during hydrate formation will be all the more valid that the amount of residual water at the end of the experiment is small.

Eq. (2) was used to calculate $\Delta n_{CO_2}^h$:

$$\Delta n_{CO_2}^h = \frac{n_{CO_2}^g(T_{targ},P)v_{CO_2}^g(T_{targ},P) + N_h n_{CO_2}^w(T_{targ},P)v_w \quad n_{CO_2}^g(T_{targ},P')v_{CO_2}^g(T_{targ},P') + n_{CO_2}^w(T_{targ},P)v_h}{v_h \quad v_{CO_2}^g(T_{targ},P') \quad N_h v_w} \tag{2}$$

where $n_{CO_2}^i$ is the number of moles of CO_2 in the gas phase ($i=g$) or the water phase ($i=w$), $v_{CO_2}^g$, v_w and v_h are the molar volumes of CO_2, water and CO_2 hydrate respectively, at the gas pressure P measured before hydrate formation or P' measured after hydrate formation, at T_{targ}.

We used in the above equation a hydration number N_h of 6.04 (Kumar et al., 2009), 18 cm^3/mol for v_w, 12 Å for the length side of the cubic sI unit crystal formed by CO_2 hydrate (Sloan and Koh, 2008) and $(N_{Avogadro}(12 \times 10^{-8})^3/46)N_h = 136.62$ cm^3 per mol of CO_2 for v_h.

$n_{CO_2}^w(T_{targ}, P)$ was calculated using a semi empirical model previously developed for determining CO_2 solubility in aqueous solutions which contain water soluble additives (Ricaurte et al., 2012).

First of all, Table 2 shows that for all systems and conditions investigated, the reproducibility of the experiments is fairly good.

On the one hand, the total pressure decrease measured at equilibrium is approximately the same for the two investigated temperatures, showing that the total amount of CO_2 hydrate formed in the SG100 porous medium is not significantly modified

by varying the hydrate formation temperature. On the other hand, the kinetics of hydrate formation is considerably affected by the temperature at which the hydrate is formed: the higher the temperature, the slower the kinetics. The trends observed here are consistent with the results published by Kang and Lee (2010) on the influence of the driving force (expressed in their work as the difference between the experimental pressure and the hydrate equilibrium pressure at the same temperature) on hydrate formation behavior for CO_2 hydrate formed in spherical silica gel of nominal pore diameter 100 nm saturated with pure water or with a 100 ppm SDS solution. These authors have shown that a high driving force (> 1 MPa) has a greater impact on the kinetics of hydrate formation than on the total amount of hydrate formed (expressed in their case in terms of total amount of CO_2 consumed). Note that in our experiments, the driving force was about 1.1 MPa at 279.2 K and 1.4 MPa at 278.2 K.

Contrary to Tween 80, SDS was observed to speed up hydrate formation in the SG100 porous medium. Yet, its kinetic effect, which is more pronounced at the higher investigated temperature, remains low compared to the effect of the temperature set to form the hydrate. For instance, adding 100 ppm of SDS to pure water produced a 6% increase in R_f at the hydrate formation temperature of 279.2 K, whereas decreasing the formation temperature by only 1 K resulted in a 30% increase of R_f.

The values of ΔP_f show that the presence of SDS slightly increases the total amount of hydrate as compared to pure water and to Tween 80. The values obtained for τ_w confirm the observed tendency and suggest that, for all conditions and systems investigated in this study, most of the water present was converted to hydrate. Kumar et al. (2013), in their recent work, found the same trend for the influence of SDS on the amount of hydrate formed, but their observations applied to systems with much higher surfactant concentrations (> 500 ppm). Moreover, they reported values for the final conversion water to hydrate molar ratio smaller than 0.52, whereas the values found in our experiments were higher than 0.90. One possible reason for this difference is that these authors assumed in their calculation that the CO_2 consumed during hydrate formation came exclusively from the gas phase, and did not take into account the reduction of the gas phase volume resulting from the water expansion during its transformation into hydrates. Using their assumptions and our experimental data, we obtained final conversion water to hydrate molar ratio varying between 0.70 (for pure water at 279.2 K) and 0.80 (for SDS at 278.2 K).

3.4. Possible action mechanisms of the additives

The difference in the amount of water converted to hydrate between the SDS system and the other systems, clearly observed at 279.2 K in our experiments, cannot be explained by a change in the experimental conditions, since they were identical for all systems (same amounts of water, gas phase and porous medium in the cell). It is well known that surfactants do not modify the equilibrium conditions of bulk hydrates. But their influence on
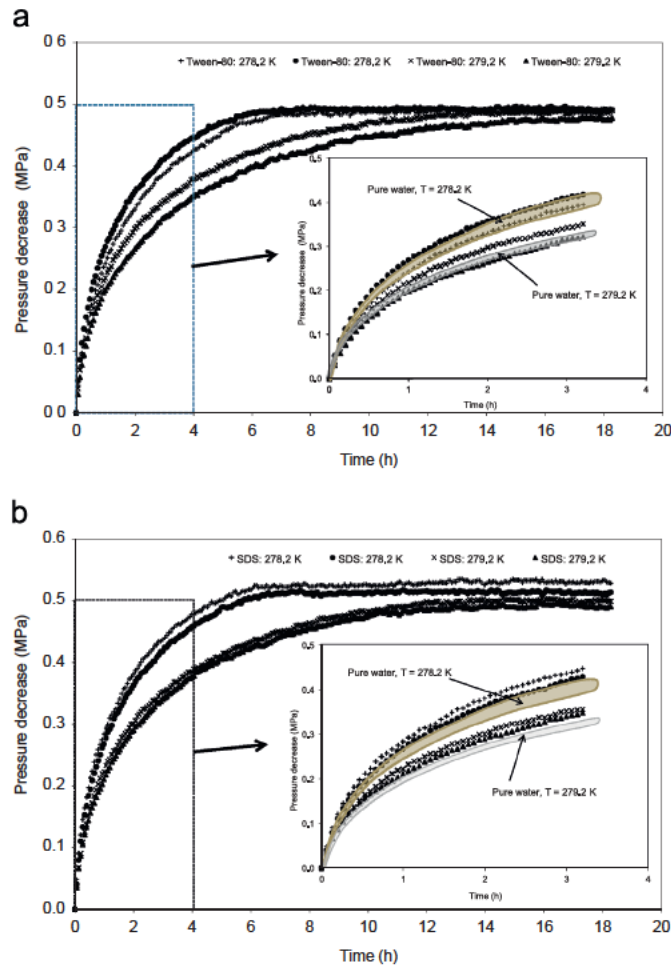
Fig. 7. Pressure decrease as a function of time for the SG100 porous medium partially (80%) saturated with a 100 ppm solution of: (a) Tween-80, and (b) SDS, at two different temperatures imposed for hydrate formation.

Table 2
Formation kinetics and equilibrium data for the CO_2-hydrate formed in the SG100 porous medium.

System	T_{exp} (K)	$t_{50\%}$ (h)	$t_{90\%}$ (h)	R_f^a (MPa/h)	ΔP_f (MPa)	τ_w (mol%)
Pure water	279.2	1.45 ± 0.02	7.7 ± 0.3	0.519 ± 0.003	0.48 ± 0.01	95 ± 2
	278.2	0.95 ± 0.01	4.20 ± 0.05	0.676 ± 0.001	0.500 ± 0.005	98 ± 2
Tween-80	279.2	1.4 ± 0.2	7.7 ± 0.7	0.51 ± 0.04	0.48 ± 0.01	94 ± 1
	278.2	0.9 ± 0.1	4.2 ± 0.4	0.66 ± 0.05	0.495 ± 0.005	100 ± 1
SDS	279.2	1.33 ± 0.05	7.2 ± 0.2	0.548 ± 0.001	0.495 ± 0.005	100 ± 1
	278.2	0.89 ± 0.02	4.2 ± 0.1	0.71 ± 0.04	0.52 ± 0.01	101 ± 1

[a] The fit of the data with a 6° polynomial gives R-squared values higher than 0.9996.

porous hydrate equilibrium conditions is not documented. The thermodynamic models developed for predicting hydrate equilibrium conditions in porous media (see for example Hashemi et al., 2012; Dicharry et al., 2005; Kang et al., 2008) generally use a correction term to take account of the capillary effect. This term is proportional to the ratio ($\sigma_{HW} \cos \theta_{HW}/r$), where σ_{HW} is the interfacial tension between the hydrate and liquid water phases, θ_{HW} the wetting angle and r the pore radius. The value of θ_{HW} is usually assumed to be 0 the water wets the hydrate and the estimated value of σ_{HW} is generally around 0.030 J/m² for CO_2 hydrate (Anderson et al., 2003). It is likely that the presence of a surfactant impacts on the values of σ_{HW} and θ_{HW}, thus modifying the hydrate equilibrium conditions in porous media. Fig. 8 shows a comparison between the CO_2 hydrate heating curves obtained with pure water and with 100 ppm of SDS in the SG100 porous medium. Because the measured hydrate dissociation temperatures are known to shift upward with the heating rate applied, and this dependency may also increase in the presence of chemicals
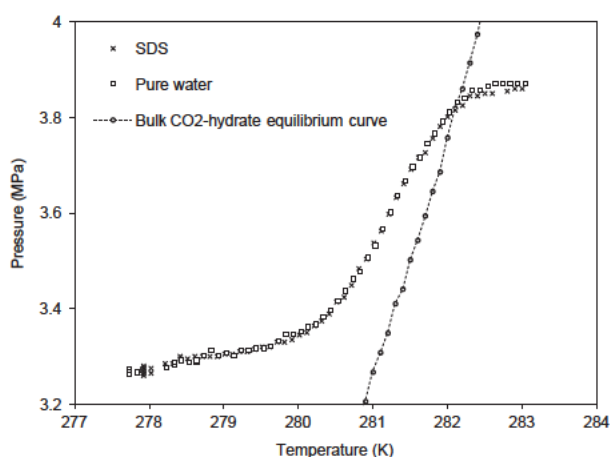
(Svartaas et al., 2008), we chose for this experiment to heat the systems at the rate of 0.05 K/h (the smallest rate possible with our experimental system) to decompose the hydrate formed.

The heating curves obtained from the two systems super impose almost perfectly, thus demonstrating that the slightly higher amount of hydrate formed in the presence of SDS is not due to a thermodynamic effect of this surfactant on CO_2 hydrate formation in the porous medium.

Another possible explanation for the higher amount of hydrate formed with SDS lies in differences in the hydrate formation behavior. In the presence of SDS, hydrates are known to form a porous layer at the w/g interface, more permeable to water and gas than the continuous solid film formed in the absence of SDS, and thus conducive to the continuation of hydrate crystallization (Gayet et al., 2005; Torré et al., 2012; Okutani et al., 2008).

In an attempt to better comprehend the effect of SDS on the formation of CO_2 hydrate in *quiescent conditions*, we performed further experiments without the porous medium and using a high pressure cell fitted with two sapphire windows (see Torré et al., 2012 for the main characteristics of this cell). Two systems were investigated: (i) pure water and (ii) water with 100 ppm of SDS, using the following experimental protocol. The cell was first loaded with 65 ± 0.1 cm³ of aqueous solution and regulated at 283.0 ± 0.2 K, purged three times with CO_2, and then progressively pressurized to 3.00 ± 0.03 MPa with CO_2. This volume of liquid was chosen in order to locate the initial w/g interface at the middle of the cell windows. The cell pressure was maintained constant while the solution was vigorously agitated with a magnetic stirrer (agitation speed set at 600 rpm) for at least 120 min in order to dissolve the CO_2 in the solution. It was then isolated from the gas supply vessel and its temperature was decreased to below 273.2 K to form hydrate. The hydrate was then decomposed at 281.8 K for 27 ± 1 min. At the end of the dissociation step, the solution was perfectly transparent (no visible hydrate particles). The agitation was then stopped and the cell was cooled to form the hydrate at a temperature arbitrarily set at 276.0 ± 0.5 K. The experiment was run until the cell pressure reached the arbitrary value of 2.64 MPa. Fig. 9 shows the variation

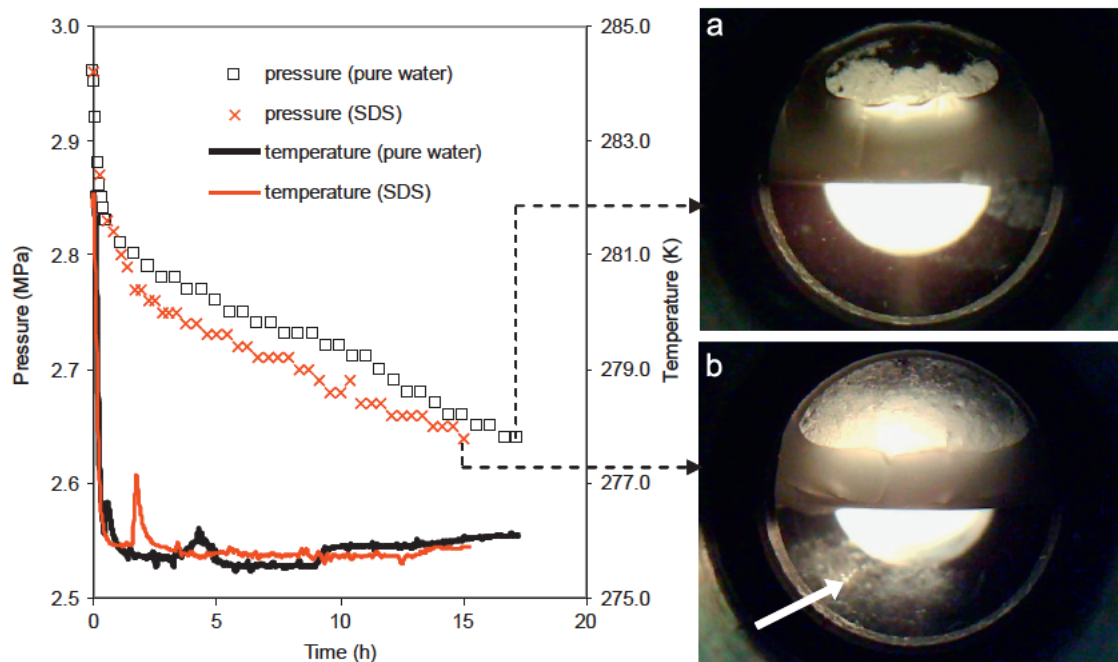**Fig. 8.** CO_2-hydrate heating curves for the SG100 porous medium with or without SDS.

Fig. 9. Cell pressure and temperature variation for bulk CO_2-hydrate formed with pure water and a solution containing 100 ppm of SDS in quiescent conditions. The hydrate formation temperature is 276.0 ± 0.5 K. Snapshots were taken at the end of the experiment when the cell pressure was equal to 2.64 MPa. The white arrow shows hydrate structures located in bulk water underneath the interfacial gas hydrate layer.

in the cell pressure and temperature obtained over the second hydrate formation step and a snapshot taken at the end of the experiment for the two systems.

The presence of SDS in the solution has no significant impact on the kinetics of CO_2 enclathration, as the trends of the two pressure curves are nearly identical. As the experiments were stopped at the same pressure (i.e. 2.64 MPa), a meaningful comparison could be made of the hydrate morphologies obtained. As shown in snapshots A and B in Fig. 9, a solid white layer of CO_2 hydrate formed at the w/g interface in both systems. The image resolution is not sufficient to identify any difference in porosity between the two layers. A thin layer of CO_2 hydrate was also observed to have formed on the top part of the cell window, but the most interesting observation we made is that, when SDS is present, CO_2 hydrate first formed in the bulk water phase before extending across the w/g interface. The hydrate crystals (white arrow in snapshot B), which are clearly located underneath the interfacial gas hydrate layer at the end of the experiment, resemble a loosely aggregated "candy floss" structure in the water phase. This structure was not observed (see snapshot A) when no SDS was present.

Our observations therefore show that SDS fosters "bulk conversion" of water to CO_2 hydrate. This property of SDS may help reach a higher level of water to hydrate conversion when SDS is present in the pore water which concurs with the results discussed in Section 3.3 of this paper.

4. Conclusion

This work evaluated the formation behavior of CO_2 hydrate in porous media of nominal pore diameter 30 nm and 100 nm, with or without a surfactant at two different temperatures. Before performing the main experiments, an experimental protocol based on the "water memory" effect was developed to precisely control the hydrate formation temperature. We found that neither of the porous media used in this study were altered by the successive hydrate formation/decomposition cycles, and the distribution of water in the pores remained unchanged, as proven by the very close match of the heating curves superimposed cycle after cycle. For the porous medium with the smallest nominal pore diameter (30 nm), the shift of CO_2 hydrate equilibrium conditions toward lower temperatures and higher pressures (as compared to bulk CO_2 hydrate) was too large to easily sustain a comparison of the hydrate formation behavior at the temperatures chosen for this study. The results obtained with the porous medium of 100 nm nominal pore diameter show that most (more than 90 mol% according to our estimation) of the water present is converted to hydrate in all investigated cases. They also confirm that combining a porous medium and a surfactant may have a positive effect on both the kinetics of hydrate formation and the amount of hydrate formed. Concerning the two surfactants tested, SDS was found to be the more effective. It does not modify CO_2 hydrate equilibrium conditions in the porous medium but, as suggested by our observations for hydrate formation in quiescent bulk systems, possibly allows the hydrate to form not only at the w/g interface (as in the absence of SDS), but also in the water phase. This would cause more of the water in the pores to be converted to hydrate when SDS is present than when it is absent.

From a practical point of view, the use of porous media in a hydrate based CO_2 capture process appears to be highly promising compared to classical bulk hydrate processes (e.g. stirred vessels). The option of combining a porous medium and a kinetic additive might further increase the water conversion to hydrate and gas enclathration kinetics, particularly when the process has to be operated close to hydrate equilibrium conditions (e.g. at relatively high temperature set point). Nevertheless, the enhancement effect obtained with kinetic additive remains relatively minor (second order) compared to that of the driving force (e.g. a small decrease of the temperature set to form hydrate).

References

Adeyemo, A., Kumar, R., Linga, P., Ripmeester, J., Englezos, P., 2010. Capture of carbon dioxide from flue or fuel gas mixtures by clathrate crystallization in a silica gel column. Int. J. Greenhouse Gas Control 4, 478–485.

Anderson, R., Llamedo, M., Tohidi, B., Burgass, R.W., 2003. Experimental measurement of methane and carbon dioxide clathrate hydrate equilibria in mesoporous silica. J. Phys. Chem. B 107, 3507–3514.

Belosludov, V.R., Subbotin, O.S., Krupskii, D.S., Belosludov, R.V., Kawazoe, Y., Kudo, J. I., 2007. Physical and chemical properties of gas hydrates: theoretical aspects of energy storage application. Mater. Trans. 48 (4), 704–710.

Darbouret, M., Cournil, M., Herri, J.-M., 2005. Rheological study of TBAB hydrate slurries as secondary two-phase refrigerants. Int. J. Refrig. 28, 663–671.

Delahaye, A., Fournaison, L., Jerbi, S., Mayoufi, N., 2011. Rheological properties of CO_2 hydrate slurry flow in the presence of additives. Ind. Eng. Chem. Res. 50, 8344–8353.

Dicharry, C., Gayet, P., Marion, G., Graciaa, A., Nesterov, A., 2005. Modeling heating curves for gas hydrate dissociation in porous media. J. Phys. Chem. B 109 (36), 17205–17211.

Duchateau, C., Peytavy, J.-L., Glénat, P., Pou, T.-E., Hidalgo, M., Dicharry, C., 2009. Laboratory evaluation of kinetic hydrate inhibitors: a procedure for enhancing the repeatability of test results. Energy Fuels 23, 962–966.

Duchateau, C., Glénat, P., Pou, T.-E., Hidalgo, M., Dicharry, C., 2010. Hydrate precursor test method for the laboratory evaluation of kinetic hydrate inhibitors. Energy Fuels 24, 616–623.

Englezos, P., Kalogerakis, N., Dholabhai, P.D., Bishnoi, P.R., 1987. Kinetics of formation of methane and ethane hydrates. Chem. Eng. Sci. 42 (11), 2647–2658.

Gayet, P., Dicharry, C., Marion, G., Graciaa, A., Lachaise, J., Nesterov, A., 2005. Experimental determination of methane hydrate equilibrium curve up to 55 MPa by using a small amount of surfactant as hydrate promoter. Chem. Eng. Sci. 60 (21), 5751–5758.

Gudmundsson, J.S., Andersson, V., Levik, O.I., Parlaktuna, M.M., 1999. Natural gas hydrates: a new gas transportation form. J. Petrol. Technol. 51 (4), 66–67.

Handa, Y.P., Stupin, D., 1992. Thermodynamic properties and dissociation characteristics of methane and propane hydrates in 70 Å-radius silica gel pores. J. Phys. Chem. 96 (21), 8599–8603.

Hashemi, H., Javanmardi, J., Zarifi, M., Eslamimanesh, A., Mohammadi, A.H., 2012. Experimental study and thermodynamic modelling of methane clathrate hydrate dissociation conditions in silica gel porous media in the presence of methanol aqueous solutions. J. Chem. Thermodyn. 49, 7–13.

Kang, S.-P., Lee, H., Lee, C.-S., Sung, W.-M., 2001. Hydrate phase equilibria of the guest mixtures containing CO_2, H_2 and tetrahydrofuran. Fluid Phase Equilib. 185 (1–2), 101–109.

Kang, S.-P., Lee, J.-W., Ryu, H.-J., 2008. Phase behavior of methane and carbon dioxide hydrates in meso- and macro-sized porous media. Fluid Phase Equilib. 274 (1–2), 68–72.

Kang, S.-P., Lee, J.-W., 2010. Kinetics behaviors of CO_2 hydrates in porous media and effect of kinetic promoter on the formation kinetics. Chem. Eng. Sci. 65 (5), 1840–1845.

Kumar, R., Lang, S., Englezos, P., Ripmeester, J., 2009. Application of the ATR-IR spectroscopic technique to the characterization of hydrates formed by CO_2, CO_2/H_2 and $CO_2/H_2/C_3H_8$. J. Phys. Chem. A 113 (22), 6308–6313.

Kumar, A., Sakpal, T., Linga, P., Kumar, R., 2013. Influence of contact medium and surfactants on carbon dioxide clathrate hydrate kinetics. Fuel 105, 664–671.

Mohammadi, A.H., Eslamimanesh, A., Belandria, V., Richon, D., Naidoo, P., Ramjugernath, D., 2012. Phase equilibrium measurements for semi-clathrate hydrates of the (CO_2+N_2+tetra-n-butylammonium bromide) aqueous solution system. J. Chem. Thermodyn. 46, 57–61.

Ohmura, R., Kashiwazaki, S., Mori, Y.H., 2000. Measurements of clathrate-hydrate film thickness using laser interferometry. J. Cryst. Growth 218 (2), 372–380.

Okutani, K., Kuwabara, Y., Mori, Y.H., 2008. Surfactant effects on hydrate formation in an unstirred gas/liquid system: an experimental study using methane and sodium alkyl sulfates. Chem. Eng. Sci 63 (1), 183–194.

Ricaurte, M., Torré, J.-P., Broseta, D., Diaz, J., Dicharry, C., Renaud, X., 2011. CO_2 removal from a CO_2–CH_4 gas mixture by hydrate formation: evaluation of additives and operating conditions. In: Proceedings of the 7th International Conference on Gas Hydrates (ICGH 2011), Edinburgh, Scotland, United Kingdom, July 17–21.

Ricaurte, M., Torré, J.-P., Asbai, A., Broseta, D., Dicharry, C., 2012. Experimental data, modeling and correlation of carbon dioxide solubility in aqueous solutions containing low concentrations of clathrate hydrate promoters: application to CO_2–CH_4 gas mixtures. Ind. Eng. Chem. Res. 51 (7), 3157–3169.

Sloan, E.D., Koh, C.A., 2008. Clathrate Hydrates of Natural Gases, third ed. CRC Press, New York.

Seo, Y.-T., Moudrakovski, I.L., Ripmeester, J.A., Lee, J.-W., Lee, H., 2005. Efficient recovery of CO_2 from flue gas by clathrate hydrate formation in porous silica gel. Environ. Sci. Technol. 39, 2315–2319.

Sun, Q., Guo, X., Liu, A., Liu, B., Huo, Y., Chen, G., 2011. Experimental study on the separation of CH_4 and N_2 via hydrate formation in TBAB solution. Ind. Eng. Chem. Res. 50 (4), 2284–2288.

Svartaas, T.M., Gulbrandsen, A.C., Fjelldal, T.H., Gjeessen, M., 2008. An experimental study on the effect of the KHI polymer size on sII hydrate formation and dissociation in an isochoric cell system. In: Proceedings of the 6th International Conference on Gas Hydrates, Vancouver, Canada, July 6–10.

Torré, J.P., Dicharry, C., Ricaurte, M., Daniel-David, D., Broseta, D., 2011. CO_2 capture by hydrate formation in quiescent conditions: in search of efficient kinetic additives. Energy Procedia 4, 621–628.

Torré, J.P., Ricaurte, M., Dicharry, C., Broseta, D., 2012. CO_2 enclathration in the presence of water-soluble hydrate promoters: hydrate phase equilibria and kinetics studies in quiescent conditions. Chem. Eng. Sci. 82, 1–13.

Turner, D.J., Cherry, R.S., Sloan, E.D., 2005. Sensitivity of methane hydrate phase equilibria to sediment pore size. Fluid Phase Equilib. 228–229, 505–510.

Zhong, Y., Rogers, R.E., 2000. Surfactant effects on gas hydrate formation. Chem. Eng. Sci. 55 (19), 4175–4187.

Zhu, C., Li, Y., Wang, W., Chen, Y., Chen, P., Liu, H., Liang, B., 2011. Effect of surfactants on the hydrate formation kinetics of carbon dioxide. In: Proceedings of the 7th International Conference on Gas Hydrates (ICGH 2011), Edinburgh, Scotland, United Kingdom, July 17–21.